Discovery of 3-Aminobenzyloxycarbonyl as an N-Terminal Group Conferring High Affinity to the Minimal Phosphopeptide Sequence Recognized by the Grb2-SH2 Domain

Pascal Furet,* Brigitte Gay, Carlos García-Echeverría, Joseph Rahuel, Heinz Fretz, Joseph Schoepfer, and Giorgio Caravatti

Novartis Pharma Inc., Oncology Research Department, CH-4002 Basel, Switzerland

Received March 31, 1997[⊗]

The observation that anthranilic acid as N-terminal group produces a dramatic increase of the binding affinity of the phosphopeptide sequence Glu-pTyr-Ile-Asn for the Grb2-SH2 domain was rationalized by molecular modeling. The model, which invokes a stacking interaction between the N-terminal group and the SH2 domain residue Arg αA2, was subsequently used to design the 3-aminobenzyloxycarbonyl N-terminal group. The latter confers high affinity (IC_{50} = 65 nM in an ELISA assay) to the minimal sequence pTyr-Ile-Asn recognized by the Grb2-SH2 domain.

Introduction

Intervention in the signal transduction pathways of tyrosine kinase growth factor receptors is a contemporary theme in anticancer drug research.[1−3] Many efforts have focused on preventing tyrosine phosphorylation and the consequent intracellular signal propagation by chemical inhibition of the kinase enzymatic activity of these receptors.[4,5] Downstream in the signaling cascade, blocking the interaction between the phosphotyrosine (pTyr)-containing activated receptors and the Src homology 2 (SH2) domain of the growth factor receptor-bound protein 2 (Grb2) constitutes another approach of potential interest in the search for new antitumor agents.[6,7] This strategy, which targets a key component of the ras activation pathway,[8,9] is conceptually attractive. Starting from the minimal peptide sequence pTyr-Ile-Asn recognized by the Grb2-SH2 domain,[10] we have initiated a medicinal chemistry project in this direction. A first objective in the project was to improve the binding affinity of the minimal sequence to progress toward the identification of low molecular weight compounds that can efficiently disrupt these protein−protein interactions. As part of this effort, we report here the rationalization by molecular modeling of the unexpected beneficial effect on affinity observed upon introduction of a particular fluorophore at the N-terminus of a Grb2-SH2 phosphopeptide ligand. We also describe how this finding has been exploited to design an N-terminal capping group of phosphotyrosine that increases the binding affinity of the unprotected minimal sequence by 3 orders of magnitude.

Results and Discussion

Anthranilic Acid Effect. To assess the binding affinity of ligands for the Grb2-SH2 domain, we have set up an ELISA-type assay that measures their ability to inhibit the binding of the phosphorylated C-terminal intracellular domain of the epidermal growth factor receptor (EGFR) to this SH2 domain.[11] In the early phase of the project, we envisaged to develop an alternative binding test based on fluorescence. For that purpose, reference phosphopeptides bearing the anthranilic acid (Abz) fluorophore at the N-terminus were synthesized. As illustrated by a comparison of the IC_{50} values of compounds **1** and **2** (Table 1), it turned out that Abz, when appended at the N-terminus of the amino acid preceding the phosphotyrosine, produced a dramatic, unexpected increase of the binding affinity of the phosphopeptides for the Grb2-SH2 domain. At the time this result was obtained, we had not yet determined the X-ray crystal structure of the Grb2-SH2 domain in complex with a phosphopeptide.[11] Still, using the available coordinates of an homologous SH2 domain, that of the protein $p56^{lck}$ (Lck) complexed with the high-affinity phosphopeptide Glu-Pro-Gln-pTyr-Glu-Glu-Ile-Pro-Ile-Tyr-Leu,[12] we could derive a hypothesis for the structural basis of this effect.

Table 1. Structure−Activity Relationships of Reported Phosphopeptides

no.	sequence	IC_{50} (μM)[a]
1	H-Glu-pTyr-Ile-Asn-NH_2	7.9 ± 0.46
2	Abz-Glu-pTyr-Ile-Asn-NH_2	0.022 ± 0.005
3	Ac-pTyr-Ile-Asn-NH_2	8.64 ± 1.56
4	H-pTyr-Ile-Asn-NH_2	56.9 ± 6.74
5	(3-amino)Z-pTyr-Ile-Asn-NH_2	0.065 ± 0.0045
6	Z-pTyr-Ile-Asn-NH_2	6.35 ± 0.59

[a] IC_{50} concentration to inhibit the binding of the phosphorylated C-terminal intracellular domain of EGFR to the Gbr2-SH2 domain.

Why the Lck Structure Is an Appropriate Model. Specificity in peptide ligands of SH2 domains is determined by the residues C-terminal to the phosphotyrosine.[13] For instance, while for the Grb2-SH2 domain an asparagine at position pTyr+2 of the sequence[14] is the dominant recognition feature, the Lck-SH2 domain preferentially binds peptides presenting the motif pTyr-Glu-Glu-Ile.[15,16] As confirmed by X-ray and NMR structural investigations,[11,12,17−19] this suggests that the three-dimensional structures of SH2 domains present significant differences in the regions involved in binding the C-terminal part ot their phosphopeptide ligands. As a corollary, because they are not critical for determining specificity, less variation is expected in the N-terminal part binding regions as well as in the phosphotyrosine recognition pockets. In particular, the analysis detailed below gave us confi-

* To whom correspondence should be addressed. E-mail: furet@chbs.ciba.com.

[⊗] Abstract published in *Advance ACS Abstracts,* September 15, 1997.

S0022-2623(97)00218-5 CCC: $14.00

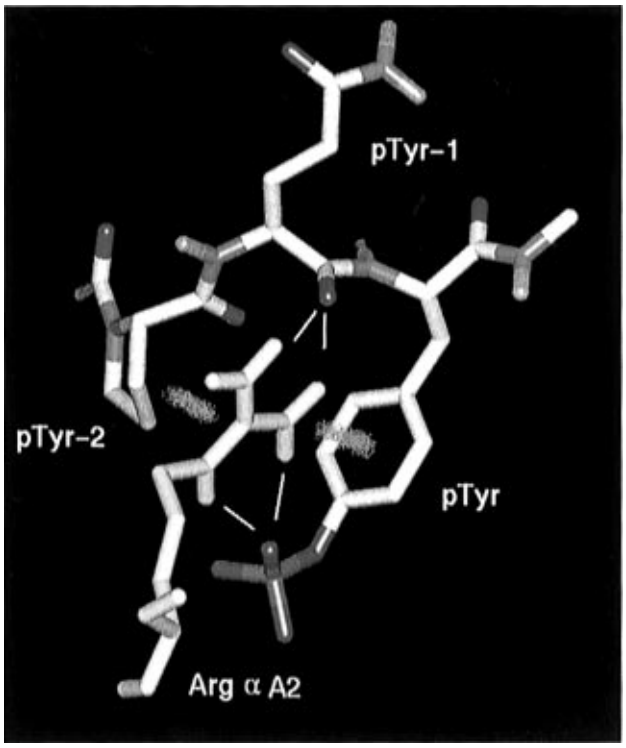

Figure 1. Interactions between residue Arg αA2 (yellow) and the phosphopeptide ligand in the Lck-SH2 domain X-ray structure. Conventional hydrogen bonds are represented as thin white lines. The amino−aromatic hydrogen bond formed with the π system of pTyr is pictured in the form of pink dots while the van der Waals contact with proline pTyr-2 as blue dots.

dence that the Lck-SH2 X-ray structure provided an appropriate frame to model the interactions between the Grb2-SH2 domain and its ligands as far as phosphotyrosine and the N-terminal residues are concerned.

According to sequence alignments,[18] the amino acids of the Lck-SH2 domain seen to interact with the ligand phosphotyrosine and its N-terminal residues in the X-ray structure are absolutely conserved in the Grb2-SH2 domain. These are Arg αA2, Arg βB5, Ser βC3, Ser BC2, Ser βB7, Lys βD6, Glu BC1, and His βD4.[21] Additional support to the notion that the three-dimensional structures of the Lck and Grb2-SH2 domains in complex with ligands are similar in this region came from structure−activity relationships reported in Table 1. In the crystal structure of the Lck-SH2 domain, the only contact existing between the glutamine pTyr-1 phosphopeptide residue and the protein is a bifurcated hydrogen bond interaction involving the ligand backbone carbonyl and the terminal nitrogens of the guanidinium moiety of Arg αA2 (see Figure 1). The side chain of the pTyr-1 residue projects away from the protein in the direction of solvent space. Consistent with the idea that a similar situation exists in ligated Grb2-SH2, comparison of the respective IC_{50} values of compounds **1**, **3**, and **4** indicates that the pTyr-1 amino acid contributes to affinity only through its backbone carbonyl function. A simple acetyl N-protection of the phosphotyrosine can replace the full pTyr-1 residue without loss of affinity (peptide **3** compared to **1**). However, removal of the protecting group causes a 7-fold increase of the IC_{50} value (peptide **4** compared to **3**) by abolishing, presumably, the hydrogen bond interaction above mentioned.

Rationalization of the Effect. Thus, taking the X-ray structure of the Lck-SH2 domain complex as a model, we sought to understand the origin of the anthranilic acid effect. The Lck structure shows that amino acid Arg αA2 makes multiple contacts with the phosphopeptide ligand. Its side chain forms hydrogen bonds with the phosphate group and, as already mentioned, the backbone carbonyl of residue pTyr-1. A less conventional amino−aromatic hydrogen bond, also seen in the structures of other SH2 domains,[22,23] is formed between the η1 nitrogen and the phosphotyrosine ring. In addition, a weak van der Waals contact exists between the guanidinium moiety and the ring of the proline residue in position pTyr-2 of the phosphopeptide sequence. These different interactions are represented in Figure 1. When the modeling experiment consisting of replacing the pTyr-2 proline residue by the Abz N-terminal group in the X-ray structure was performed, it immediately suggested a reason why this structural change could lead to a gain in binding affinity. As depicted in Figure 2, constructing Abz at the location of the proline ring in the X-ray structure followed by energy minimization places the N-terminal group in an optimal position to make a favorable planar π-π stacking interaction with the guanidinium moiety of Arg αA2. Stacking interactions between arginine side chains and aromatic or heteroaromatic moieties have often been observed in structural biology,[24] and calculations on model complexes suggest that they can produce substantial stabilization energy.[25] In fact, statistical analysis of protein structures indicates that arginine and aromatic amino acid side chains interact more frequently in the stacked geometry than in the perpendicular (amino−aromatic hydrogen bond) one.[25] Stacking gives to an arginine guanidinium group that has fulfilled its hydrogen bonding potential, as it is the case for Arg αA2, an additional possibility of interaction. Recently, this type of interaction between an electron-rich aromatic moiety and the electron-poor guanidinium group has also been invoked to rationalize the structure−activity relationships of some matrix metalloproteinase inhibitors.[26] To check if other low-energy binding geometries could exist, a local Monte Carlo search of the conformations accessible to the N-terminal part of the Abz-protected phosphopeptide ligand in complex with the Lck-SH2 domain was carried out. The conformation corresponding to the stacking interaction between Abz and Arg αA2 came out as the global minimum, reinforcing the plausibility of our hypothesis regarding the origin of the anthranilic acid effect.

As can be seen in Figure 2, in our model of the complex in which Abz stacks on Arg αA2, the 2-amino substituent of the protecting group is within hydrogen-bonding distance of one of the pTyr phosphate oxgen atoms. We speculated that this intramolecular hydrogen bond in the ligand, by locking its N-terminal part in the conformation recognized by the SH2 domain, also contributed to the exceptional increase in affinity conferred by Abz.

Design of a 3-Aminobenzyloxycarbonyl N-Terminal Group. As discussed in the preceding sections, the side chain of the ligand pTyr-1 amino acid does not contribute to affinity. According to our model, the glutamic acid pTyr-1 residue of **2**, apart from its main chain carbonyl group, acts as a neutral spacer connect-

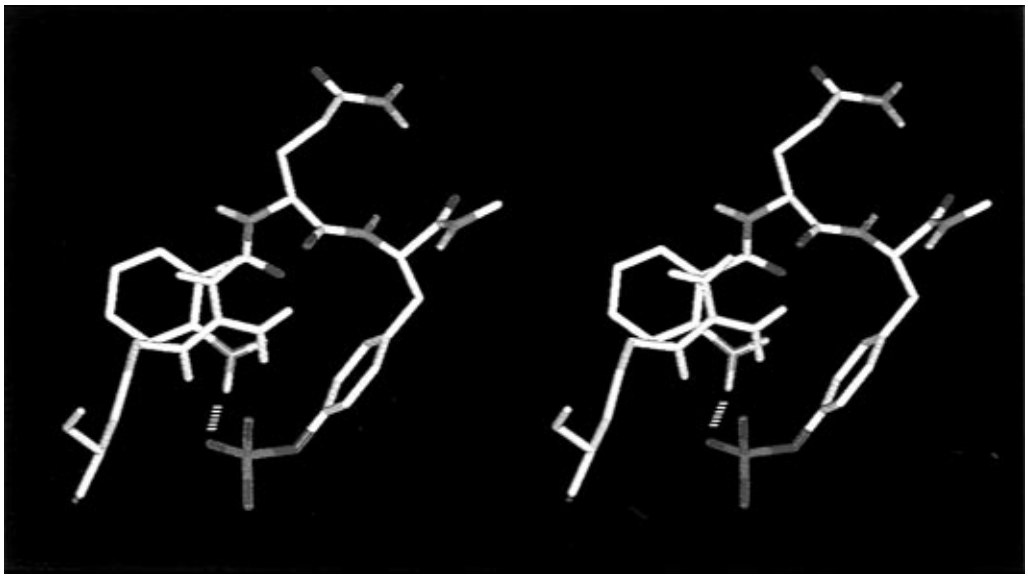

Figure 2. Model (stereoview) of the stacking interaction between the phosphopeptide Abz N-terminal group and the SH2 domain residue Arg αA2 (yellow). The hydrogen bond between the 2-amino substituent of Abz and the phosphate group of pTyr is represented as a dashed line.

ing the important pTyr and Abz moieties. This suggested that it should be possible to design an appropriate N-terminal group that could mimic the stacking interaction of Abz and be directly attached to the phosphotyrosine, thus eliminating one unnecessary amino acid in potent compound **2**.

Inspection of the model in Figure 2 revealed that the part of the Abz group in contact with the guanidinium moiety of Arg αA2 extends beyond the phenyl ring. It also includes a surface patch belonging to the atoms forming the pseudo-six-membered ring resulting from the intramolecular hydrogen bond between the 2-amino substituent and the carbonyl group (Abz was constructed in this conformation as described in the molecular modeling part of the Experimental Section). An electrostatic potential map of the Abz fragment (Figure 3) clearly shows that the electron-rich region corresponding to negative values of the molecular electrostatic potential and having affinity for the electron-poor guanidinium group is centered in the middle of the bicyclic system formed by the phenyl and the pseudo-six-membered rings. Interactive modeling work suggested that the phenyl ring of a 3-amino-substituted benzyloxycarbonyl (Z) group, appended at the N-terminus of phosphotyrosine, could appropriately mimic the bicycle-centered part of Abz in contact with the guanidinium moiety of Arg αA2 without compromising the other ligand-SH2 domain interactions. The resulting energy-minimized model is shown in Figure 4.

The synthetic realization of this idea, compound **5**, confirmed the validity of the design. With an IC_{50} value of 65 nM (Table 1), **5** is almost equipotent to **2** while being one amino acid residue shorter. Three orders of magnitude in binding affinity were gained with respect to the unprotected reference tripeptide sequence **4**.

To assess the importance of the 3-amino substituent in producing this dramatic increase in affinity, **6**, the unsubstituted Z-protected analogue of **5,** was also synthesized. As shown in Table 1, the amino substituent is essential. No gain in affinity was obtained with **6** compared to the acetyl-protected peptide **3.** In the model, the most obvious role of the amino substituent

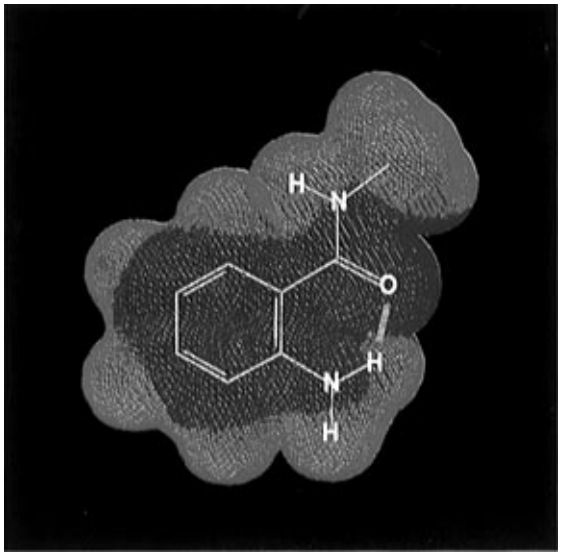

Figure 3. Electrostatic potential map of the Abz N-terminal group. The electrostatic potential is displayed as isovalue contour lines on the van der Waals surface of the molecule (negative values, blue; positive values, red). The intramolecular hydrogen bond formed by the 2-amino substituent and the carbonyl group appears as a dashed line.

is to lock the N-terminal part of the peptide in the stacking conformation by forming a strong intramolecular hydrogen bond with the charged phosphate group of pTyr. However, the electron-donating property of the substituent, by increasing the electronic density on the phenyl ring of Z with the result of strengthening the interaction with the electron-deficient arginine guanidinium group, is very likely to also have a contribution to the enhancement of affinity. Thus, the large increase in potency induced by Abz or its (3-amino)Z mimetic seems to depend on the synergy between an enthalpic ($\pi-\pi$ stacking strengthened by an electron-donating substituent) and an entropic (conformational restriction by an internal hydrogen bond) favorable effect.

Repeating the modeling work above described using our recently solved X-ray crystal structure of the Grb2-SH2 domain[11] gave the same results in accordance with

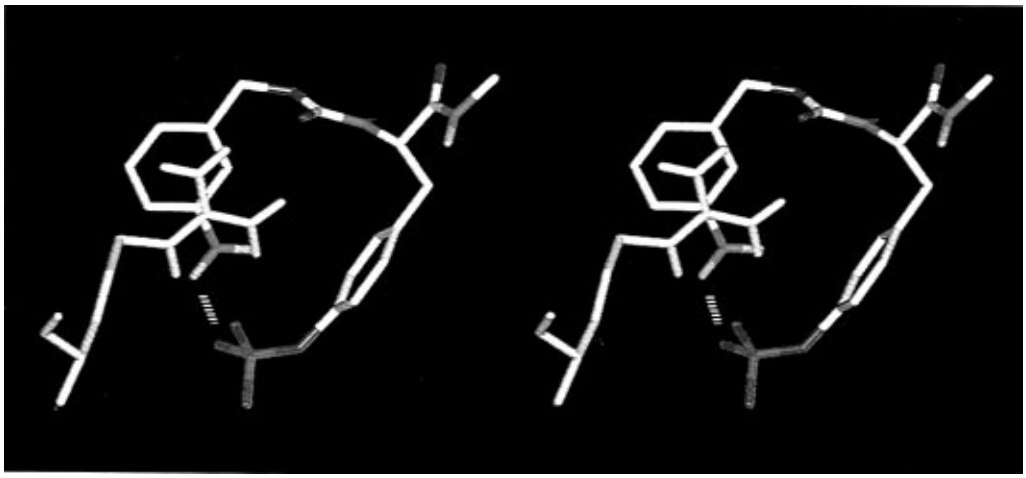

Figure 4. Model (stereoview) of the stacking interaction between the designed phosphopeptide (3-amino)Z N-terminal group and the SH2 domain residue Arg αA2 (yellow). The hydrogen bond between the 3-amino substituent of the N-terminal goup and the phosphate moiety of pTyr is represented as a dashed line.

the expected high degree of similarity observed between the Lck and Grb2-SH2 structures in the region of the phosphotyrosine binding pocket.

Conclusion

Molecular modeling based on the X-ray structure of an SH2 domain homologue to that of Grb2 allowed us to formulate a hypothesis regarding the structural basis of the anthranilic acid effect discovered by serendipity.

The resulting model was successfully used to design an N-terminal capping group of phosphotyrosine that can impart high affinity to the minimal tripeptide sequence recognized by the Grb2-SH2 domain. The small size and the high potency of the phosphopeptide thus obtained represent a major advance in the search for low molecular weight compounds that can block a crucial protein−protein interaction in the signal transduction pathways of tyrosine kinase growth factor receptors.

Since the anthranilic acid effect is assumed to originate in an interaction with the well-conserved Arg αA2 amino acid, it should also be observed for SH2 domains other than Grb2. We are currently in the process of checking this idea by applying the same N-terminal modifications to phosphopeptide sequences specific to various other SH2 domains

Experimental Section

4-[[[(2′,4′-Dimethoxyphenyl)Fmoc]amino]methyl]phenoxy]-polystyrene resin (1% DVB cross-linked, 0.4 mequiv/g, 100−200 mesh) and BOP and HOBt reagents were purchased from NovaBiochem (Läufelfingen, Switzerland). TPTU reagent was from Senn Chemicals AG (Dielsdorf, Switzerland). HATU reagent was from PerSeptive Biosystems (Hamburg, Germany). The required Fmoc derivatives were obtained using standard protocols. N^{α}-Fmoc-Tyr(PO_3H_2)-OH was synthesized as described previously.[27] 2-Aminobenzoic acid, trifluoroacetic acid, diisopropylethylamine, and piperidine were from Fluka (Buchs, Switzerland). *N*,*N*-Dimethylacetamide was from Merck (Hohenbrunn, Germany) and *N*-methylpyrrolidin-2-one was from SDS (Peypin, France). All commerical chemicals used were of the highest quality available (AR grade or higher).

3-[*N*-*tert*-Butoxycarbonyl)amino]benzyl Alcohol. Di-*tert*-butyl dicarbonate (13.4 mL, 60 mmol) was added to a solution of 3-aminobenzyl alcohol (2.46 g, 20 mmol) in THF:1 N NaOH (125 mL, 1:1, v/v), and stirring was continued until completion of the reaction. The alkaline solution was extracted with petroleum ether (2 × 25 mL); the ether extracts were discarded. The aqueous phase was acidified with a 5% solution of citric acid and extracted with ethyl acetate (3 × 30 mL). The ethyl acetate extracts were pooled, washed with water (3 × 30 mL), dried over anhydrous Na_2SO_4, and evaporated in vacuo. Yield: 4.0 g (18 mmol, 90%). TLC: $R_f = 0.72$ (chloroform:methanol:water:acetic acid = 750:270:50:5, v/v/v/v). ^{1}H NMR (CD_3OD): δ 1.50 (s, 9H, *t*-Bu), 4.56 (s, 2H), 6.98 (d, J = 7.5 Hz, 1H), 7.21 (t, J = 7.5 Hz, 1H), 7.30 (d, J = 7.5 Hz, 1H), 7.40 (s, 1H).

3-[*N*-(*tert*-Butoxycarbonyl)amino]benzyl 4-Nitrophenyl Carbonate. A solution of 3-[*N*-(*tert*-butoxycarbonyl)amino]-benzyl alcohol (1.0 g, 4.5 mmol) in anhydrous pyridine (18 mL) was cooled in an ice−water, bath and 4-nitrophenyl chloroformate (0.9 g, 4.5 mmol) was added with stirring. The solution was stirred for 17 h at room temperature and then added to a mixture of diisoporpyl ether/petroleum ether (1:1, v/v; 200 mL). The ether mixture was extracted with brine (1 × 50 mL) and then with water (7 × 50 mL), dried over anhydrous Na_2SO_4, and evaporated *in vacuo*. The crude compound was purified by flash chromatography on silica gel, using dichloromethane as eluent. Yield: 1.25 g (3.2 mmol, 71%). Mp: 93.3−94.3 °C. TLC: R_f = 0.66 (chloroform/methanol = 95:5, v/v). MS: *m*/*z* 387 (M − H). ^{1}H NMR ($CDCl_3$): δ 1.52 (s, 9H, *t*-Bu), 5.28 (s, 2H), 6.55 (s, 1H, NH), 7.10 (d, J = 7.5 Hz, 1H), 7.30 (m, 2H), 7.40 (d, J = 7.5 Hz, 2H), 7.58 (s, 1H), 8.38 (d, J = 7.5 Hz, 2H).

Peptide Synthesis. Peptides **1**, **5**, and **6** were synthesized manually on a 4-[[(2′,4′-dimethoxyphenyl)amino]methyl]-phenoxy resin,[28] employing the fluorenylmethoxycarbonyl strategy. Fmoc-removal was with piperidine/DMA (1:4, v/v; 6 × 2 min), followed by washing with MeOH (3 × 1 min), NMP (2 × 1 min), MeOH (3 × 1 min), and NMP (3 × 2 min). The required Fmoc derivatives of asparagine, isoleucine, and glutamic acid were incorporated using their 2,4,5-trichlorophenyl esters (2 equiv) in the presence of HOBt (2 equiv) and DIEA (0.75 equiv). Asparagine and glutamic acid side chains were protected with the trityl and the *tert*-butyl group, respectively. The incorporation of N^{α}-Fmoc-Tyr(PO_3H_2)-OH (3 equiv)[27,29] was accomplished with BOP/HOBt (1:1; 3 equiv; first coupling)[30] and HATU (3 equiv; second coupling)[31] in the presence of DIEA (7 equiv). 3-[*N*-(*tert*-Butoxycarbonyl)amino]-benzyl 4-nitrophenyl carbonate (3 equiv) was coupled to the N-terminal residue of the peptide resin (peptide **5**) in the presence of an equimolar amount of DIEA in NMP during 17 h at room temperature. Benzyl chloroformate (3 equiv) was coupled to the N-terminal residue of the peptide resin (peptide **6**) in the presence of DIEA (6 equiv) in NMP during 17 h at room temperature.

Peptides **2**−**4** were synthesized on a Milligen 9050 automated peptide synthesizer, starting with an Fmoc-PAL-PEG-

resin[32] for establishing the C-terminal carboxamide, and using chemical protocols based on the fluorenylmethoxycarbonyl chemistry. The required Fmoc-amino acids (3 equiv) were coupled using their 2,4,5-trichlorophenyl esters (single coupling) with minimum reaction times of 30 min. The amino acid side chains are protected as described above. Double coupling with TPTU (3 equiv)[33] was carried out for glutamic acid (peptide **2**). The incorporation of N^{α}-Fmoc-Tyr(PO_3H_2)-OH (3 equiv) was accomplished with BOP/HOBt (1:1; 3 equiv; first coupling) and HATU (3 equiv; second coupling) in the presence of DIEA (6 equiv). 2-Aminobenzoic acid (peptide **2**) was incorporated with BOP/HOBt as described above. 3-[*N*-(*tert*-Butoxycarbonyl)amino]benzyl 4-nitrophenyl carbonate (3 equiv) was coupled manually to the N-terminal residue of the peptide resin (peptide **5**) in the presence of an equimolar amount of DIEA in NMP during 17 h at room temperature

The complete peptide resins obtained after the last coupling step were simultaneosly deprotected and cleaved by treatment with TFA/H_2O (95:5, v/v) for 3 h at room temperature. The filtrate from the cleavage reaction was precipitated in diisopropyl ether/petroleum ether (1:1, v/v, 0 °C), and the precipitate was collected by filtration. The crude peptides were purified by medium-pressure liquid chromatography using a C_{18}-column (Merck LICHROPREP RP-18, 15−25 μm bead diameter; detection at 215 nm) eluted with an acetonitrile−water gradient containing 0.1% of TFA. Fractions shown by HPLC to be >95% pure were pooled and lyophilized to provide the title compounds as white powder TFA salts. Mass-spectral analysis (MALDI-TOF) revealed a molecular mass within 0.1% of the expected value (negative-ion mode): 615.9 (**1**, calcd 615.6, $C_{24}H_{36}N_6O_{11}P_1$); 734.5 (**2**, calcd 734.7, $C_{31}H_{41}N_7O_{12}P_1$); 528.8 (**3**, calcd 528.5, $C_{21}H_{31}N_5O_9P_1$); 486.4 (**4**, calcd 486.5, $C_{19}H_{29}N_5O_8P_1$); 635.7 (**5**, calcd 635.6, $C_{27}H_{36}N_6O_{10}P_1$); 620.8 (**1**, calcd 620.6, $C_{27}H_{35}N_5O_{10}P_1$). The purity of the peptide was verified by reversed-phase analytical HPLC on a Nucleosil C_{18}-column (250 × 4 mm, 5 μm, 100 Å): (A) linear gradient over 10 min of MeCN/0.09% TFA and H_2O/0.1% TFA from 5:95 to 65:35; (B) linear gradient over 10 min of MeCN/0.09% TFA and H_2O/0.1% TFA from 1:49 to 3:2; (C) linear gradient over 10 min of MeCN/0.09% TFA and H_2O/0.1% TFA from 1:49 to 2:3, flow rate 2.0 mL/min, detection at 215 nm; single peak at t_R = 4.20 min (**1**, A); t_R = 5.38 min (**2**, B); t_R = 5.62 min (**3**, C); t_R = 3.99 min (**4**, C); t_R = 5.54 min (**5**, B); t_R = 7.37 min (**6**, B). Identical results were obtained by capillary electrophoresis (Beckmann, P/ACE System 5000): normal capillary 75 μm × 50 cm, sodium phosphate 0.05 M (pH 9.3) and/or sodium tetraborate 0.05 M (pH 9.3), 10 min at 25 kV, detection at 214 nm, T = 23 °C.

Abbreviations. Abbreviations for amino acids and nomenclature of peptides structures follow the recommendations of the IUPAC−IUB Commission on Biochemical Nomenclature (*Eur. J. Biochem.* **1984**, *138*, 9). Other abbreviations are as follows: Abz, anthranilic acid or anthranilamide; Fmoc, 9-fluorenylmethyloxycarbonyl; HATU, *N*-[[(dimethylamino)-1*H*-1,2,3-triazolo[4,5-*b*]pyridin-1-yl]methylene]-*N*-methylmethanaminium hexafluorophosphate *N*-oxide; Boc, *tert*-butyloxycarbonyl; BOP, (1*H*-benzotriazol-1-yloxy)tris(dimethylamino)phosphonium hexafluorophospahte; DIEA, diisopropylethylamine; DMA, *N*,*N*-dimethylacetamide; HOBt, 1-hydroxybenzotriazole; HPLC, high-performance liquid chromatography; PAL, tris(alkoxy)benzylamide linker; PEG, poly(ethylene glycol); NMR, nuclear magnetic resonance; MALDI-TOF, matrix-assisted laser-desorption ionization time-of-flight mass spectrometry; NMP, *N*-methylpyrrolidin-2-one; R_f, ratio of fronts in thin layer chromatogrphy employing silica gel plates; TFA, trifluoroacetic acid; THF, tetrahydrofuran; TLC, thin layer chromatography; TPTU, 2-(2-oxo-1(2H)-pyridyl)-1,1,3,3-tetramethyluronium tetrafluoroborate; pTyr, phosphotyrosine; t_R, retention time.

Cloning and Expression of Recombinant Proteins. Glutathione S-transferase (GST) fusion proteins of Grb2 (GST/Grb2-SH2) were from Santa Cruz Biotech. The pMAL-c2 expression vector (New England Biolabs) was used to express the C-terminal domain of the epidermal growth factor receptor intracellular domain (residues 976−1210) as a maltose-binding fusion protein (MBP-EGFR) in *Escherichia Coli*. Two oligodeoxy ribonucleotides were prepared on an automated Applied Biosystems Model 392 DNA synthesizer, using phosphoramidite chemistry: (A) 5′-tata*gaattc*cagcgctaccttgctattcagggg-3′; (B) 5′-TATA*AAGCTT*TCATGCTCCAATAAATTCACTGC-TTTG-3′. (A) + (B) were used as PCR primers to amplify segments of the human EGFR cDNA sequence corresponding to nucleotides 3112−3816. The PCR fragment was cleaved with *Eco*RI and *Hind*III from Boehringer Mannheim before it was ligated with *Eco*RI + *Hind*III-cleaved pMal-C2 DNA. The ligation was used to transform *E. coli* SURE competent cells (Stratagene) and transformants were selected at 37 °C on LB agar plates supplemented with 100 g/mL ampicillin. Plasmid DNA was isolated from individual ampicillin-resistant colonies and analyzed by restriction endonuclease digestion to identify the desired recombinants. Expression of the MBP-EGFR fusion protein was performed essentially according to New England Biolabs protocols.

EGFR Assay. The assay has already been described elsewhere.[11] Briefly, phosphorylated MBP-EGFR immobilized on a solid phase (polystyrene microtiter plates, NUNC MAXYSORB) was incubated with a GST/Grb2-SH2 fusion protein capable of binding to it, in the presence of a phosphopeptide or buffer. Bound SH2 was detected with polyclonal rabbit anti-GST antibody. Following washing, horse raddish peroxidase-conjugated mouse anti-rabbit antibody was added. Peroxydase activity is monitored at 655 nm on a plate reader by adding 100 L/well of a solution of tetramethylbenzidine as substrate.

Data Analysis. Peptide inhibitors effects were calculated as a percentage of the reduction in absorbance in the presence of each peptide inhibitor concentration compared to absorbance obtained with GST/SH2 in the absence of peptide inhibitor. Dose−response relationships were constructed by nonlinear regression of the competition curves with Grafit (Erithacus Software, London, U.K.). Fifty percent inhibitory (IC_{50}) concentrations were calculated from the regression lines.

Molecular Modeling. The following methods as implemented in MacroModel v.4.0[34] were used: (i) energy minimization with the AMBER[35] force field (dielectric constant of 4*r* for the electrostatics), (ii) conformational search with the Monte Carlo/energy minimization procedure[36] (advanced protocol), (iii) calculation and display of electrostatic potential on the molecular van der Waals surface[37] employing MNDO[38] (Mulliken population analysis) atomic charges computed with the program MOPAC v.6.0.[39]

In the Figure 2 model, Abz was constructed in the conformation presenting an intramolecular hydrogen bond between the 2-amino substituent and the carbonyl group as observed in the X-ray crystal structures of small organic molecules containing this moiety (Cambridge crystallographic database[40] codes JEGSOD and JIXCIC). In the Monte Carlo search and minimizations, only the water molecules seen to mediate hydrogen bonds between the ligand and the Lck-SH2 domain in the X-ray structure were kept. The ligand, these water molecules as well as the protein residues within a distance of 5 Å of the initial position of the ligand were allowed to move freely upon energy minimization, while those at a distance between 5 and 8 Å were constrained by application of a parabolic force constant of 50 kJ/Å. Residues beyond 8 Å were ignored. The Monte Carlo search consisted of 5000 steps where the main chain angle of pTyr and all the torsion angles of Abz and the pTyr-1 amino acid were taken as variables. The conformation of the (3-amino)Z N-terminal group in the model of Figure 4 was calculated to be of low energy as confirmed by its occurrence in the X-ray crystal structure of a Z-protected peptide molecule (Cambridge crystallographic database[40] code SIDWIL).

Figures 1, 2, and 4 were prepared in Insight II (MSI corporation, San Diego, CA).

Acknowledgment. The authors are grateful to R. Wille, D. Arz, V. von Arx, and C. Stamm for their technical assistance and to S. E. Shoelson for providing the coordinates of the Lck-SH2 domain X-ray structure.

References

(1) Gibbs, J. B.; Oliff, A. Pharmaceutical Research in Molecular Oncology. *Cell* **1994**, *79*, 193−198.

(2) Saltiel, A. R; Sawyer, T. K. Targeting Signal Transduction in the Discovery of Antiproliferative Drugs. *Chem. Biol.* **1996**, *3*, 887−893.

(3) Levitzki, A. Signal Transduction Therapy. A Novel Approach to Disease Management. *Eur. J. Biochem.* **1994**, *226*, 1−13.

(4) Groundwater, P. W.; Solomons, K. R. H.; Drewe, J. A.; Munawar, M. A. Protein Tyrosine Kinase Inhibitors. In *Progress in Medicinal Chemistry*; Ellis, G. P., Luscombe, D. K., Eds.; Elsevier Science B. V.: Amsterdam, 1996; Vol. 33, pp 233−329.

(5) Traxler, P.; Lydon, N. Recent Advances in Protein Tyrosine Kinase Inhibitors. *Drugs Future* **1995**, *20*, 1261−1274.

(6) Gishizky, M. L. Tyrosine Kinase Induced Mitogenesis Breaking the Link with Cancer. In *Annual Reports in Medicinal Chemistry*; Bristol, J. A., Ed.; Academic Press: San Diego, 1995; Vol. 30, pp 247−253.

(7) Smithgall, T. E. SH2 and SH3 Domains: Potential Targets for Anti-Cancer Drug Design. *J. Pharmacol. Toxicol. Methods* **1995**, *34*, 125−132.

(8) Lowenstein, E. J.; Daly, R. J.; Batzer, W. L.; Margolis, B.; Lammers, R.; Ullrich, A.; Skolnik, E. Y.; Bar-Sagi, D.; Schlessinger, J. The SH2 and SH3 Domain-Containing Protein Grb2 Links Receptor Tyrosine Kinases to ras Signaling. *Cell* **1992**, *70*, 431−442.

(9) Rojas, M.; Yao, S. Y.; Lin, Y. Z. Controlling Epidermal Growth Factor (EGF)-stimulated Ras Activation in Intacts Cells by a Cell-permeable Peptide Mimicking Phosphorylated EGF Receptor. *J. Biol. Chem.* **1996**, *271*, 27456−27461.

(10) Peptide studies have established that the minimal sequence retaining micromolar affinity for the Grb2-SH2 domain is the tripeptide pTyr-Ile-Asn. Asparagine at position pTyr+2 is absolutely required while the pTyr+1 position is more versatile, valine, glutamine and glutamic acid being good substitutes for isoleucine (Garcia-Echeverria, C.; et al. Novartis Pharma Inc., Oncology Research Department, unpublished results).

(11) Rahuel, J.; Gay, B.; Erdmann, D., Strauss, A.; Garcia-Echeverria, C.; Furet, P.; Caravatti, G.; Fretz, H.; Schoepfer, J.; Gruetter, M. Structural Basis for Specificity of Grb2-SH2 Revealed by a Novel Ligand Binding Mode *Nature Struct. Biol.* **1996**, *3*, 586−589.

(12) Eck, M. J.; Shoelson, S. E.; Harrison, S. C. Structure of the Regulatory Domains of the Src-Family Tyrosine Kinase Lck. *Nature* **1993**, *362*, 87−91.

(13) Birge, R. B.; Hanafusa, H. Closing in on SH2 Specificity. *Science* **1993**, *262*, 1522−1524.

(14) Ligand residues are numbered relative to the position of the phosphotyrosine which is denoted pTyr 0.

(15) Songyang, Z.; Shoelson, S. E.; McGlade, J.; Olivier, P.; Pawson, T.; Bustelo, X. R.; Barbacid, M.; Sabe, H.; Hanafusa, H.; Yi, T.; Ren, R.; Baltimore, D.; Ratnofsky, S.; Feldman, R. A.; Cantley, L. C. Specific Motifs Recognized by the SH2 Domains of Csk, 3BP2, fps/fes, GRB-2, HCP, SHC, Syk and Vav. *Mol. Cell.Biol.* **1994**, *14*, 2777−2785.

(16) Songyang, Z.; Shoelson, S. E.; Chaudhuri, M.; Gish, G.; Pawson, T.; Hase, W.G.; King, F.; Roberts, T.; Ratnofsky, S.; Lechleider, R. J.; Neel, B. G; Birge, R.B.; Fajardo, J. E.; Chou, M. M; Hanafusa, H.; Schaffhausen, B.; Cantley, L. C. SH2 Domains Recognize Specific Phosphopeptide Sequences. *Cell* **1993**, *72*, 767−778.

(17) Pascal, S. M.; Singer, A. U.; Gish, G; Yamazaki, T.; Shoelson, S. E.; Pawson, T.; Kay, L. E.; Forman-Kay, J. D. Nuclear Magnetic Resonance Structure of an SH2 Domain Of Phospholipase C-g1 Complexed with a High Affinity Binding Peptide. *Cell* **1994**, *77*, 461−472.

(18) Lee, C. H.; Kominos, D.; Jacques, S.; Margolis, B.; Schlessinger, J.; Shoelson, S. E.; Kuriyan, J. Crystal Structures of Peptide Complexes of the Amino-Terminal SH2 Domain of the Syp Tyrosine Phosphatase. *Structure* **1994**, *2*, 423−438.

(19) Narula, S. S.; Yuan, R. W.; Adams, S. E.; Green, O. M.; Green, J.; Philips, T. B.; Zydowsky, L. D.; Botfield, M. C.; Hatada, M.; Laird, E. R.; Zoller, M. J.; Karas, J. L.; Dalgarno, D. C. Solution Structure of the C-terminal SH2 Domain of the Human Tyrosine Kinase Syk Complexed with a Phosphotyrosine Pentapeptide. *Structure* **1995**, *3*, 1061−1073.

(20) Breeze, A. L.; Kara, B. V.; Barratt, D. G.; Anderson, M.; Smith, J. C.; Luke, R.W.; Best, J. R.; Cartlidge, S. A. Structure of a Specific Peptide Complex of the Carboxy-Terminal SH2 Domain from the p85a Subunit of Phosphatidylinositol 3-Kinase. *EMBO J.* **1996**, *15*, 3579−3589.

(21) For the nomenclature of the SH2 domain residues, see ref 12 or 18.

(22) Waksman, G.; Kominos, D.; Robertson, S. C.; Pant, N.; Baltimore, D.; Birge, R. B.; Cowburn, D.; Hanafusa, H.; Mayer, B. J.; Overduin, M.; Resh, M. D.; Rios, C. B.; Silverman, L.; Kuriyan, J. Crystal Structure of the Phosphotyrosine Recognition Domain SH2 of v-*src* Complexed with Tyrosine-Phosphorylated Peptides. *Nature* **1992**, *358*, 646−653.

(23) Hatada, M. H.; Lu, X.; Laird, E. R.; Green, J.; Morgenstern, J. P.; Lou, M.; Marr, C. S.; Phillips, T. B.; Ram, M. K.; Theriault, K.; Zoller, M. j.; Karas, J. L. Molecular Basis for the Interaction of the Protein Tyrosine Kinase ZAP-70 with the T-cell Receptor. *Nature* **1995**, *377*, 32−38.

(24) Flocco, M. M.; Mowbray, S. L. Planar Stacking Interactions of Arginine and Aromatic Side-Chains in Proteins. *J. Mol. Biol.* **1994**, *235*, 709−717.

(25) Mitchell, J. B. O.; Nandi, C. L.; McDonald, I. K.; Thornton, J. M.; Price, S. L. Amino/Aromatic Interactions in Proteins: Is the Evidence Stacked Against Hydrogen Bonding? *J. Mol. Biol.* **1994**, *239*, 315−331.

(26) Gowravaram, M. R.; Tomczuk, B. E.; Johnson, J. S.; Delecki, D.; Cook, E. R.; Ghose, A. K.; Mathiowetz, A. M.; Spurlino, J. C.; Rubin, B.; Smith, D. L.; Pulvino, T.; Wahl, R. C. Inhibition of Matrix Metalloproteinase by Hydroxamates Containing Heteroatom-Based Modifications of the P_1' Group. *J. Med.Chem.* **1995**, *38*, 2570−2581.

(27) Ottinger, E. A.; Shekels, L. L.; Bernlohr, D. A.; Barany, G. Synthesis of Phosphotyrosine-Containing Peptides as Their Use as Substrates for Protein Tyrosine Phosphatases. *Biochemistry* **1993**, *32*, 4354−4361.

(28) Rink, H. Solid-Phase Synthesis of Protected Peptide Fragments Using a Trialkoxy-diphenyl-methylester resin. *Tetrahedron Lett.* **1987**, *28*, 3787−3790.

(29) For a study on the coupling of N^{α}-Fmoc-Tyr(PO_3H_2)-OH, see: García-Echeverría, C. *Lett. Pept. Sci.* **1995**, *2*, 369−373.

(30) (a) Castro, B.; Dormoy, J. R.; Evin, G.; Selve, C. Reactifs de couplage peptidique IV (1) - L′ hexafluorophosphate de benzotriazolyl N-oxytrisdimethylamino phosphonium (B.O.P.). *Tetrahedron Lett.* **1975,** *14*, 1219−1922. (b) König, W.; Geiger, R. Eine neue methode zur synthese von peptiden: aktivierung der caboxylgruppe mit dicyclohexylcarbodiimid unter zusatz von 1-hydoxy-benzotriazolen. *Chem. Ber.* **1970**, *103*, 788−798.

(31) Carpino, L. A. 1-Hydroxy-7-azabenzotriazole. An Efficient Peptide Coupling Additive. *J. Am. Chem. Soc.* **1993**, *115*, 4397−4398.

(32) Albericio, F.; Kneib-Cordonier, N.; Biancalana, S.; Gera, L.; Masada, R. I.; Hudson, D.; Barany, G. Preparation and Application of the 5-(4-(9-fluorenylmethyloxycarbonyl)aminopmethyl-3,5-dimethoxyphenoxy)-valeric Acid (PAL) Handle for the Solid-Phase Synthesis of C-Terminal Peptide Amides under Mild Conditions. *J. Org. Chem.* **1990**, *55*, 3730−3743.

(33) Knorr, R.; Trzeciak, A.; Bannwarth, W.; Gillessen, D. New Coupling Reagents in Peptide Chemistry. *Tetrahedron Lett.* **1989**, *30*, 1927−1930

(34) Mohamadi, F.; Richards, N. G.; Guida, W. C.; Liskamp, R.; Lipton, M.; Caufield, C.; Chang, G.; Hendrickson, T.; Still, W. C. Macromodel- An Integrated Software System for Modeling Organic and Bioorganic Molecules Using Molecular Mechanics. *J. Comput. Chem.* **1990**, *11*, 440−467.

(35) Weiner, S. J.; Kollman, P.; Case, D. A.; Singh, U. C.; Ghio, C.; Alagona, S.; Profeta, S.; Weiner, P. A Force Field for the Simulation of Nucleic Acids and Proteins. *J. Am. Chem. Soc.* **1984**, *106*, 765−770.

(36) Chang, G.; Guida, W. C.; Still, W. C. An Internal Coordinate Monte Carlo Method for Searching Conformational Space. *J. Am. Chem. Soc.* **1989**, *111*, 4379−4386.

(37) "In-house" addition to MacroModel: (a) Bohacek, R. S.; Guida, W. C. A Rapid Method for the Computation, Comparison and display of Molecular Volumes. *J. Mol. Graph.* **1989**, *7*, 113−117. (b) Eyraud, V.; Dietrich, A. Novartis Pharma Inc. Unpublished results.

(38) Dewar, M. J. S.; Thiel, W. Ground States of Molecules. 38. The MNDO Method. Approximation and Parameters. *J. Am. Chem. Soc.* **1977**, *99*, 4899−4907.

(39) Stewart, J. J. P. MOPAC. A Semiempirical Molecular Orbital Program. *J. Comput.-Aided. Mol. Des.* **1990**, *1*, 1−105.

(40) Allen, F. H.; Bellard, S.; Brice, M. D.; Cartwright, B. A.; Doubleday, A.; Higgs, H.; Hummelink, T.; Hummelink-Peters, B. G.; Kennar, O.; Motherwell, W. D. S.; Rodgers, J. R.; Watson, D. G. The Cambridge Crystallographic Database. *Acta Crystallogr.* **1979**, *B39*, 2331−2339.

JM9702185